CDF/ANAL/CALORIMETRY/CDFR/949
May 29, 1989

Energy Scale Difference between West and East FHA Calorimeters (Status Report)

T.Kamon

Abstract

We have checked a gain difference between West and East FHA calorimeteres. The result is the gain on East side is higher that on West side by 11.2 ± 6.1 % for muons and 13.7 ± 10.7 % from dijet p_T balancing study. This may be explained by a temperature difference between West and East sides, which turns out to be 15 % of gain difference. The correction multipliers for FHA energy scales of West and East calorimeters are estimated to be 1.059 ± 0.043 (*stat.*) and 0.947 ± 0.034 (*stat.*), respectively.

1 Introduction

As reported in Ref. [1], a possible gain difference between West and East FHA calorimeters was seen from dijet p_T balancing study. The gain on East side seems to be higher by 13.7 % $\pm$ 10.7 % (*stat.*) than that on West side. However, the statistics was not enough for concluding the existence of the gain difference.

Therefore, we have looked into the response for muons on FHA calorimeter as the other way of checking the difference. The forward muon data sample was given by Karen Byrum.[1]

2 Event Selection and Analysis

The analysis was done with a standard set of analysis modules:

VTVERT CALORIMETRY[2] CLEANUP[3] FMDTE FMTRK FMOCR FMUMON[4]

Event selection in our analysis is described below.

Initial Event Selection

The initial event selection for this study was made by requiring the following conditions.

- $\mid Z_{vertex} \mid \leq 60$ cm.
- A fiducial cut for the muon position: 1-19, 66-84 in η-index of TOWE bank, where the index is given in FMUO bank.

Our analysis started with a total of 702 events after the initial event selection.

Dead Layer Correction

The FHA calorimeter has a total of 27 layers of chambers. Several quadrants have a few dead chambers due to a problem on HV. The correction of response for muon was made quadrant by quadrant as

$$E_{corr} = DLC \times E_{uncorr} \ , \tag{1}$$

where

$$DLC = \frac{27}{27 - N_{dead}} \ . \tag{2}$$

Here N_{dead} is the number of dead chambers on each quadrant. The information of the dead chambers was read out from data base once a run.

[1] Most of events in the sample were taken during months of November and December.

[2] Pedestal shift correction was enabled. A new FHA energy scale (in V5.1) was used.

[3] FHA_NCABLE and FILT_GAS were enabled.

[4] This is our own analysis module.

Clustering

The energy depositted by a muon is simply calculated to be sum energy over 3 by 3 towers ($\equiv E_{3\times3}$) on the forward calorimeter (*i.e.* FEM+FHA) around muon position. Figure 1(a) shows a correlation plot of energies on FEM and FHA calorimeters ($\equiv E_{FEM}$ and E_{FHA}, respectively). The pojections are shown in Figs. 1(b) and 1(c). Here

$$E_{3\times3} = E_{FEM} + E_{FHA} \ , \tag{3}$$

and E_{FHA} is corrected on dead layers. Figure 1(d) shows the number of towers with visible TOWE energy in 3 by 3 towers ($\equiv N^{tower}_{3\times3}$). In order to remove zero-energy cluster, we choose clusters with $1 \leq N^{tower}_{3\times3} \leq 5$. Also $N^{tower}_{3\times3(FEM)} \geq 1$ and $N^{tower}_{3\times3(FHA)} \geq 1$ are required.

Isolation

We also calculated sum energy over 5 by 5 towers ($\equiv E_{5\times5}$) and looked at an energy isolation to select a good muon candidate. Figure 2(a) shows a scatter plot of $\triangle E$ vs $E_{3\times3}$, where

$$\triangle E = E_{5\times5} - E_{3\times3} \ . \tag{4}$$

Figures 2(b) - 2(d) are the distributions of $E_{3\times3}$ in different ranges of $\triangle E$: (b) $0-2\ GeV$, (c) $2-4\ GeV$, and (d) $\geq 4\ GeV$. We see a deterioration of peak of the distribution as the value of $\triangle E$ increases. If the entries with $E_{3\times3} \geq 6\ GeV$ are taken to be background[5], the fraction of the entries to all entries are (b) 9.5 %, (c) 20 %, and (d) 25 %, respectively. This increase of the fraction is an indication of contamination of background to muon sample we want. The value of $\triangle E$ is required to be 2 GeV or less to select our "*golden*" muon events. Finally, a total of 188 events pass through all selection criteria above.

3 Result

3.1. Response for muons

A general look of our "*golden*" muons is given in Figs. 3 $\sim$ 4: Figures 3(a), 3(b), and 3(c) are a scatter plot of E_{FHA} vs E_{FEM}, E_{FHA} and E_{FEM} distributions, respectively. Figure 3(d) shows a correlation of E_{FHA} and muon momentum (in $\log_{10}$). Figure 4(a) shows the muon position given in FMUO bank after the selection. Figures 4(b) and 4(c) show plots of E_{FHA} as a function of ϕ and η, respectively.

Distributions of E_{FHA} for West and East calorimeters are shown in Figs. 5(a) and 5(b). The correlations of E_{FHA} and momentum for West and East calorimeters are also shown in Figs. 5(c) and 5(d), respectively. Note 2 peaks are seen in Fig. 5(a) on West side. There is no correlation with momentum and muon position. As mentioned later, the peaks

[5]Here, background means noise, muon associated with other particles (probablly jet), and so on.

exist for all 4 quadrants of West calorimeter. The reason is unknown at this moment.

The average response for muons is calculated to be the trancated mean values (at 6 GeV) of the distributions. We obtained:

$$FHA\ West: \quad 2.77\ GeV \quad \pm 0.100\ GeV\ (stat.)$$
$$FHA\ East: \quad 3.08\ GeV \quad \pm 0.129\ GeV\ (stat.)$$

Thus, the response on East side is higher by 11.2 % $\pm$ 6.1 % than that on West side. The value is consistent with the number (13.7 % $\pm$ 10.7 %) from dijet p_T balancing study [1].

Figures 6(a)-6(h) show distributions of E_{FHA} for 8 quadrants, separately. There seem to be 2 peaks for all 4 quadrants (Figs. 6(a)-6(d)) on West side, but it is hard to conclude the existence with this statistics.

For the sake of a systematic checkout, we summarize the mean value of response on each quadrant with the batch number of FHA chamber production in Table 1. It is seen that the mean values for 4 quadrants on each side are same each other within the statistical errors (except for Quadrant # 2 of West calorimeter). There is, however, no systematic correlation between muon response and the chamber production.

Table 1. Response for muons on each quadrant

Quad. #	Production #	Response for Muons (GeV)	# Events (after trancated)
0	7	2.75 $\pm$ 0.15	35
1	8	2.55 $\pm$ 0.24	26
2	4	3.11 $\pm$ 0.23	23
3	3	2.70 $\pm$ 0.17	22
4	6	3.01 $\pm$ 0.52	33
5	1	3.07 $\pm$ 0.27	22
6	2	3.30 $\pm$ 0.45	8
7	5	3.11 $\pm$ 0.28	16

Note that the number of events on East side (= 79 events) is less than that on West side (= 106 events). This is because of a difference in trigger efficiencies between West and East forward muon chamber systems in this data sample [2].

3.2. Relativistic rise of energy loss

In this analysis, we have to be careful for relativistic rise of energy loss in gas. Figure 7 shows a relativistic rise of the energy loss in argon [3]. For muons, the scale for π is useful. The energy loss seems to be constant for $p \geq 30\ GeV/c$. In other words, the energy loss is

rapidly changing between 10 and 20 GeV/c. Our muon sample is a biased-data with p_T: $\geq$ 10 GeV/c and $p_T \geq 1$ GeV/c as shown in Fig. 8. Therefore, we looked at the muon peak with $p \geq 30$ GeV/c (not p_T). The trancated mean values (at 6 GeV) of the distributions are:

$$\begin{aligned} FHA\ West: &\quad 2.74\ GeV \quad \pm 0.113\ GeV\ (stat.) \\ FHA\ East: &\quad 3.04\ GeV \quad \pm 0.135\ GeV\ (stat.) \end{aligned}$$

The response on East side is higher by 11.0 % $\pm$ 6.7 % than that on West side. Thus, we do not see any systematic change due to low momentum muons. Therefore, we used data sample without muon momentum cut for a final conclusion.

3.3. Correction factors

We calculate correction (multiplier) factors for West and East calorimeters by

$$C_W = \frac{0.5 \times (FHA_{East} + FHA_{West})}{FHA_{West}}, \tag{5}$$

$$C_E = \frac{0.5 \times (FHA_{East} + FHA_{West})}{FHA_{East}}. \tag{6}$$

The correction factors for FHA calorimeters are summarized in Table 2. Again, the numbers obtained from jet and muon data agree well each other. The combined numbers are also tabulated in Table 2.

Table 2. Correction factors for FHA energy scales on West and East sides

Data samples	C_W	C_E
JET_20,_40,_60	1.068 $\pm$ 0.053	0.940 $\pm$ 0.041
Muons	1.056 $\pm$ 0.031	0.950 $\pm$ 0.025
Muons+Jets	1.059 $\pm$ 0.043	0.947 $\pm$ 0.034

3.4. Why do we see such a difference ?

One possible source is a difference in room temperature between West and East sides in the collision hall. According to gas gain data, in which temperature (T) and pressure (P) data are also available, the temperature on East side is measured to be high [4]:

$$\Delta T = T_{East} - T_{West} = 4.98 \pm 0.62\ (\sigma) \tag{7}$$

In the gas gain monitoring system of the CDF gas calorimeters, the gas gain fluctuation ($\Delta G/G$) in the CDF gas calorimeter system is expressed with the fluctuation of gas density ($\Delta\rho/\rho$) as follows [5]:

$$\begin{aligned} \frac{\Delta G}{G} &= 8.9 \times (\Delta\frac{1}{\rho})/(\frac{1}{\rho}) \\ &= 8.9 \times \frac{\Delta T}{T} \end{aligned} \tag{8}$$

The second relation is obtained by assuming the pressure to be unform in the collision hall. If one put $T = 290°K$ and $\triangle T = 4.98°K$, the gas gain difference is expected to be

$$\frac{\triangle G}{G} = 0.15\,. \tag{9}$$

Therefore, one might expect the gain difference seen with data (*i.e.* jets and muons) is mainly from the temperature difference.

For FEM, however, the trancated mean values (at 2 GeV) of the distributions are:

$$\begin{array}{rll} FEM\ West: & 0.74\,GeV & \pm\ 0.041\,GeV\ (stat.) \\ FEM\ East: & 0.75\,GeV & \pm\ 0.043\,GeV\ (stat.) \end{array}$$

The responses on West and East sides are same within the statistical errors. This is consistent with the fact of no separate peaks in Z mass distribution.

At this moment, we do not know why this temperature difference does not effect FEM gas gains. Any way, for FHA, the temperature effect is most likely to cause the gain difference between West and East sides.

4 Conclusion

We conclude that the difference in the energy scale between West and East FHA calorimeters is seen with both dijet and muon data. Both results are consistent with each other. It is also consistent with the number expected from a temperature difference between West and East sides. The correction multiplier for the energy scale for West (East) calorimeter is 1.059 (0.947) $\pm$ 0.043 (0.034). The error is statistical only.

Acknowledgement

We thank K.Byrum and S.Behrends for helping the setup of analysis of the forward muon data.

References

[1] Y.Funayama, T.Kamon, T.Hessing, "Forward-Central Dijet p_T Balancing and FHA Energy Scale", CDF Note 923 (1989).

[2] K.Byrum, private communication. During the months of November and December, a few octants on East side were dead or very inefficient.

[3] F.Sauli, "Principles of Operation of Multiwire Proportional and Drift Chambers", CERN/77-09 (1977).

[4] T.Hessing, private communication. The data used in his analysis were taken during months of March and April. A total number of points were 4289.

[5] The information was given by Gas Gain group (M.Gold).

Figure Captions

Figure 1. (a) Correlation plot of E_{FHA} and E_{FEM} which are sum eneries over 3 by 3 towers on FHA and FEM around muon position, respectively.
(b) E_{FHA} distribution.
(c) E_{FEM} distribution.
(d) Number of towers with visible TOWE energy in 3 by 3 towers.

Figure 2. (a) Scaller plot of $\triangle E$ vs $E_{3\times3}$. Here $\triangle E = E_{5\times5} - E_{3\times3}$. And $E_{n\times n}$ is sum energy over 3 by 3 towers, where n is 3 or 5.
(b) $E_{3\times3}$ distribution with $0 \leq \triangle E < 2\ GeV$.
(c) $E_{3\times3}$ distribution with $2 \leq \triangle E < 4\ GeV$.
(d) $E_{3\times3}$ distribution with $\triangle E \geq 4\ GeV$.

Figure 3. Plot-(I) for "*golden*" muon events:
(a) Scatter plot of E_{FHA} vs E_{FEM}.
(b) E_{FHA} distribution.
(c) E_{FEM} distribution.
(d) Correlation of E_{FHA} and muon momentum in $\log_{10}$ scale.

Figure 4. Plot-(II) for "*golden*" muon events:
(a) Muon position in ϕ- and η-indecies.
(b) Plot of E_{FHA} as a function of ϕ-index.
(c) Plot of E_{FHA} as a function of η-index.

Figure 5. Plot-(III) for "*golden*" muon events:
(a) E_{FHA} distribution on West side.
(b) E_{FHA} distribution on East side.
(c) Correlation plot of E_{FHA} and muon momentum on West calorimeter.
(d) Correlation plot of E_{FHA} and muon momentum on East calorimeter.

Figure 6. Plot-(IV) for "*golden*" muon events:
(a)-(h) E_{FHA} distributions for 8 quqdrants, separately.

Figure 7. Relativistic rise of energy loss in argon.

Figure 8. p_T distribution of muons:
(a) all events.
(b) "*golden*" events.

Figures 1(a) – 1(d) 24-MAY-1989 10:33

#21013 FHAD(Y) VS FEM(X) (ALL)

(a)

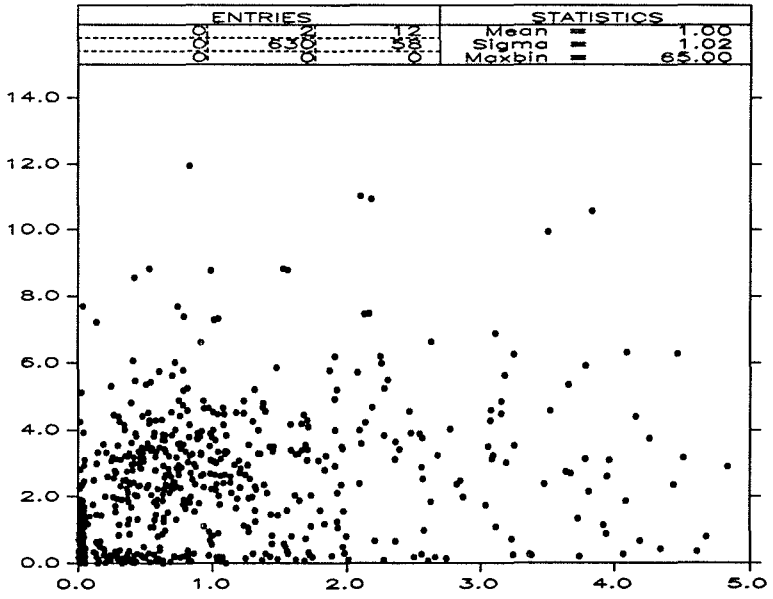

#21012 FHAD DISTRIBUTION (ALL)

(b)

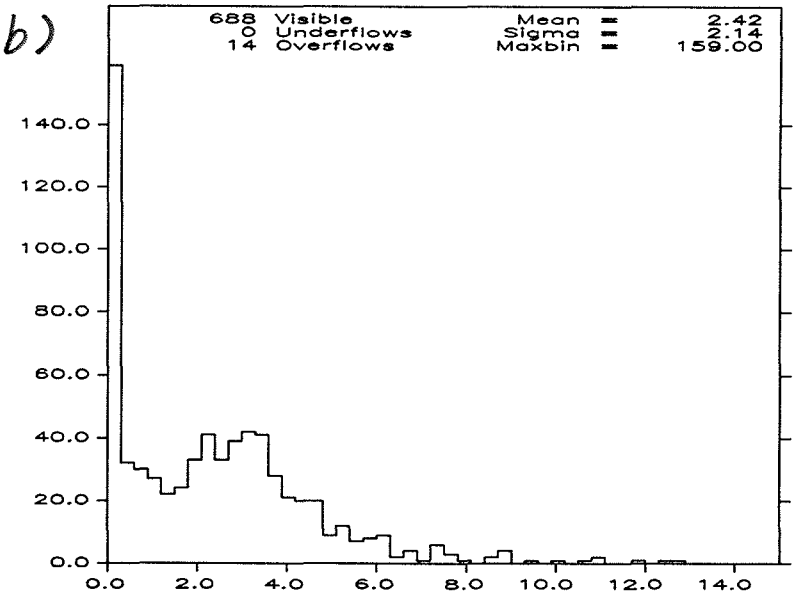

#21011 FEM DISTRIBUTION (ALL)

(c)

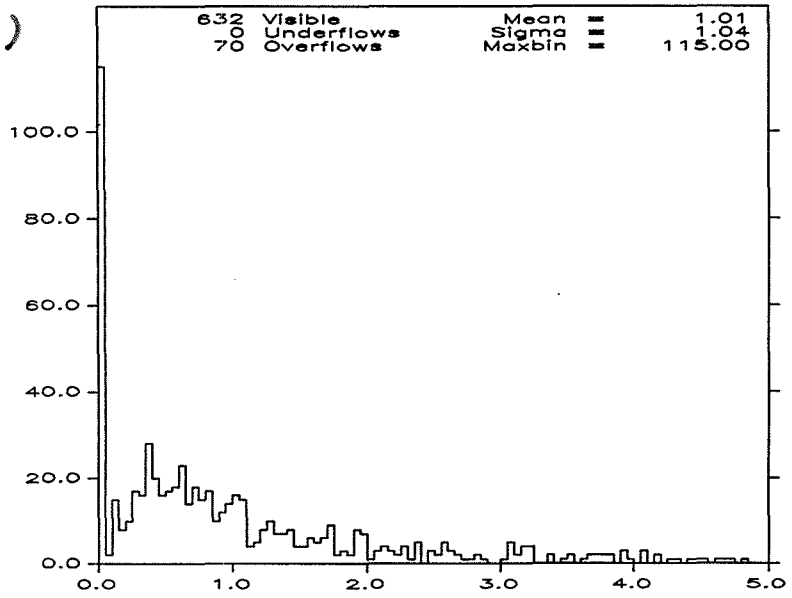

#21014 EM+HAD TOWER MULTIPLICITY (ALL)

(d)

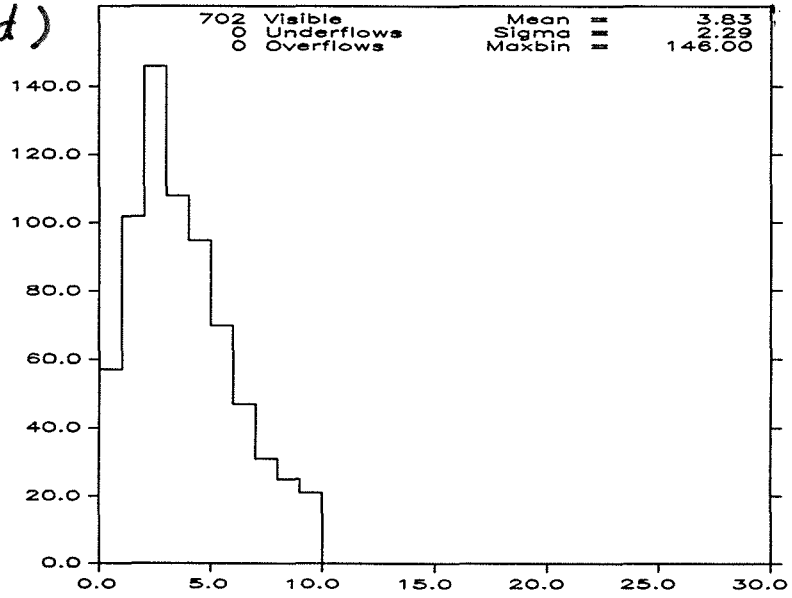

Figures 2(a) – 2(d) 24-MAY-1989 10:35

#21031 E(5X5)-E(3X3) VS E(3X3)

(a)

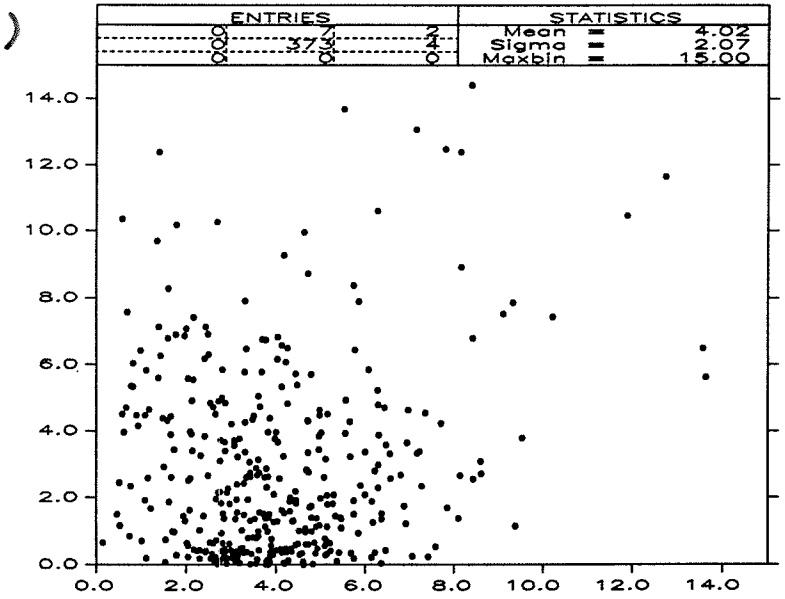

#21032 E(3X3) WITH E(BORD)=0-2 GEV

(b)

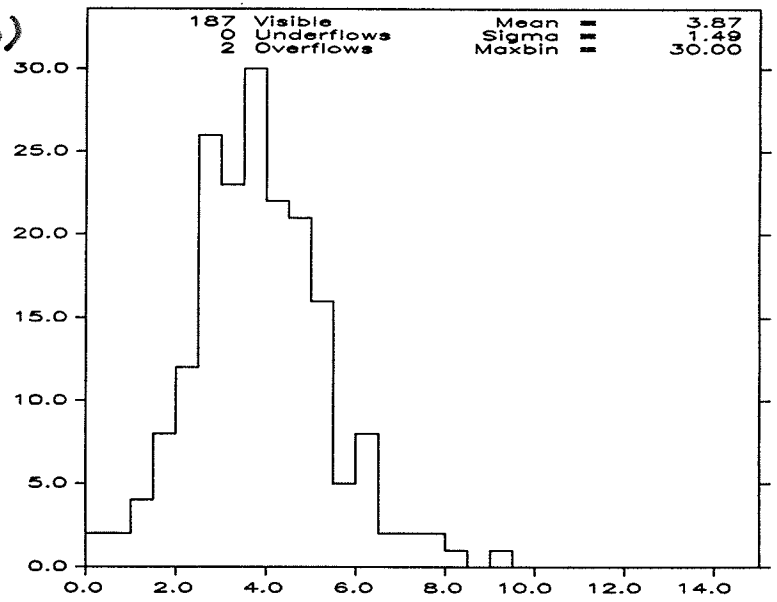

#21033 E(3X3) WITH E(BORD)=2-4 GEV

(c)

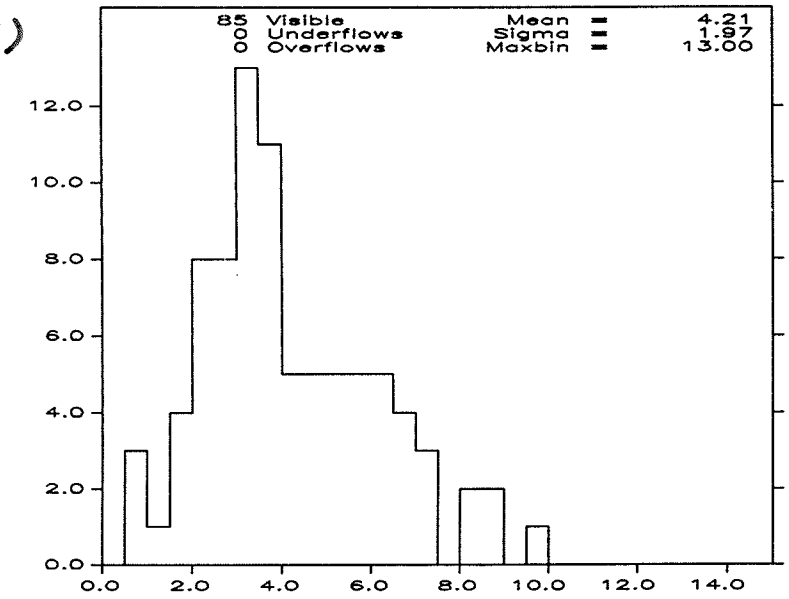

#21034 E(3X3) WITH E(BORD)=4-* GEV

(d)

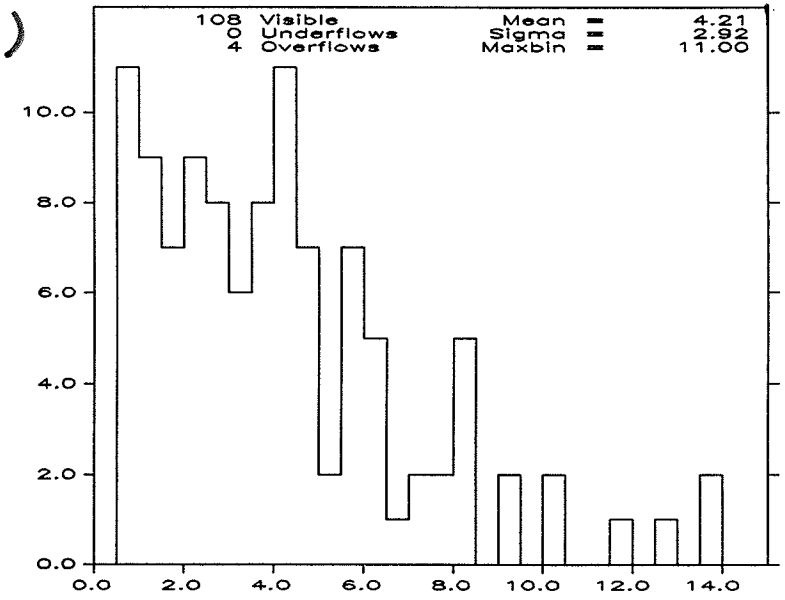

Figures 3(a) – 3(d) 24-MAY-1989 10:38

#21018 FHAD(Y) VS FEM(X) (W/CUT)

(a)

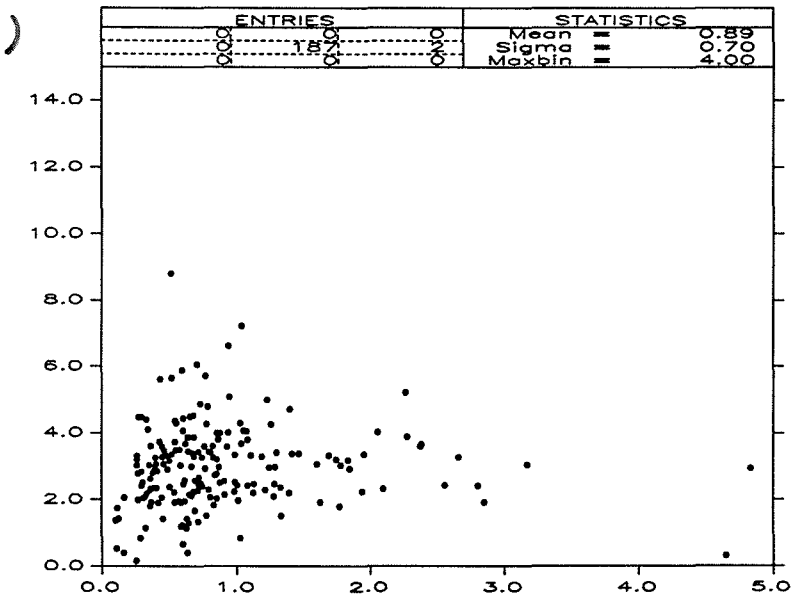

#21017 FHAD DISTRIBUTION (W/CUT)

(b)

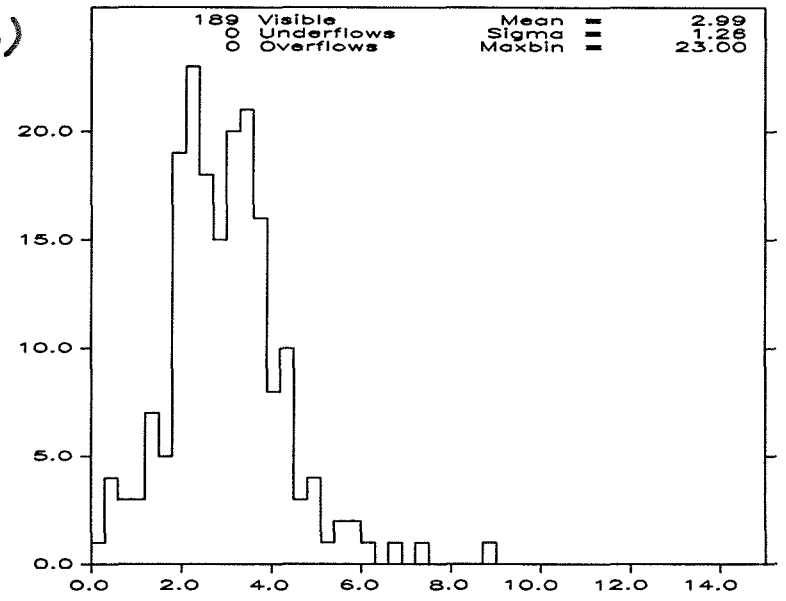

#21016 FEM DISTRIBUTION (W/CUT)

(c)

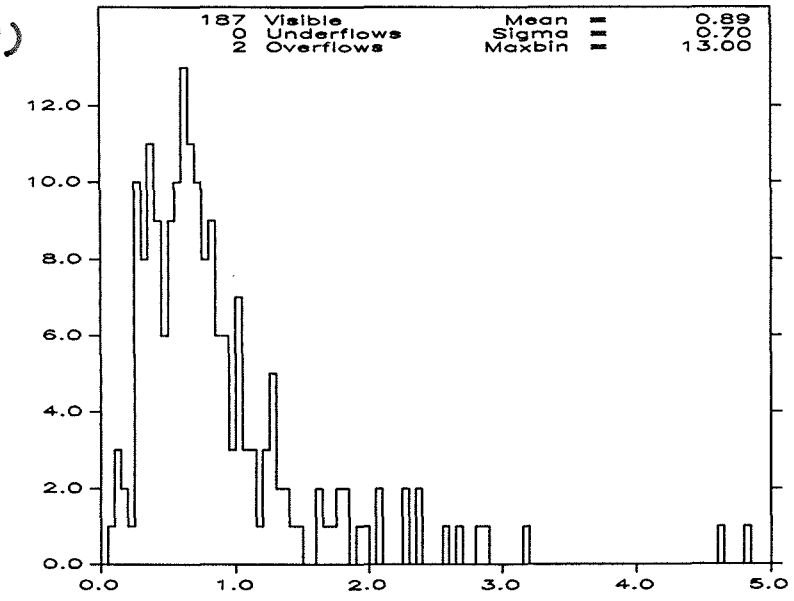

#21038 FHA VS P(MUON) (W/CUT)

(d)

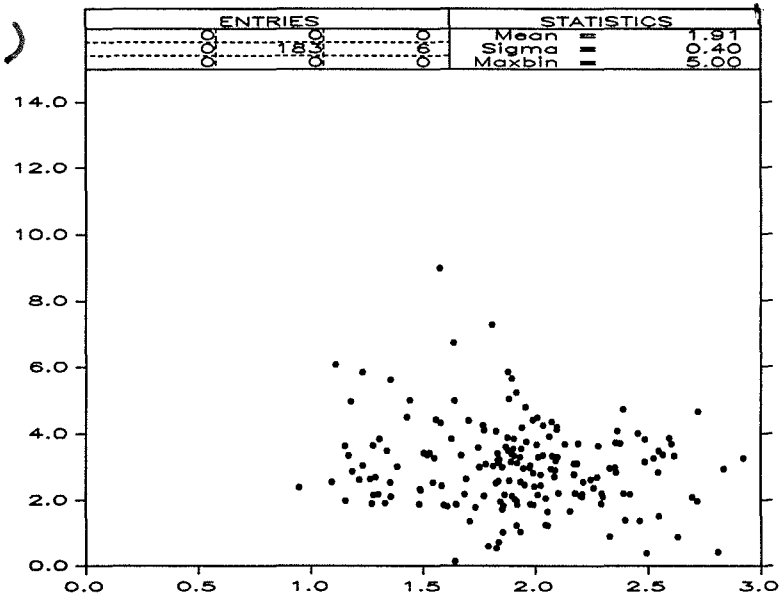

Figures 4(a) – 4(c) 24-MAY-1989 10:39

#21019 IPHI(Y) VS IETA(X) ON HAD (W/CUT)

(a)

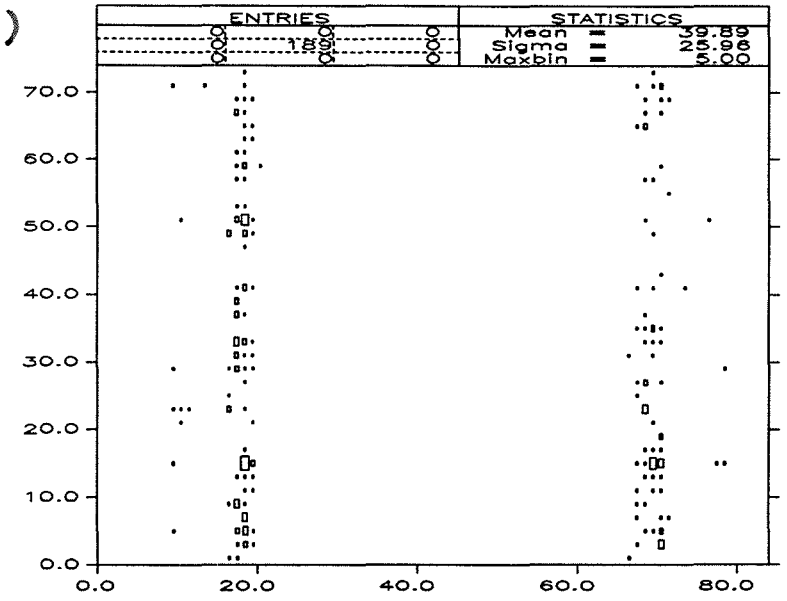

#21021 FHA(Y) VS PHI(X) (W/CUT)

(b)

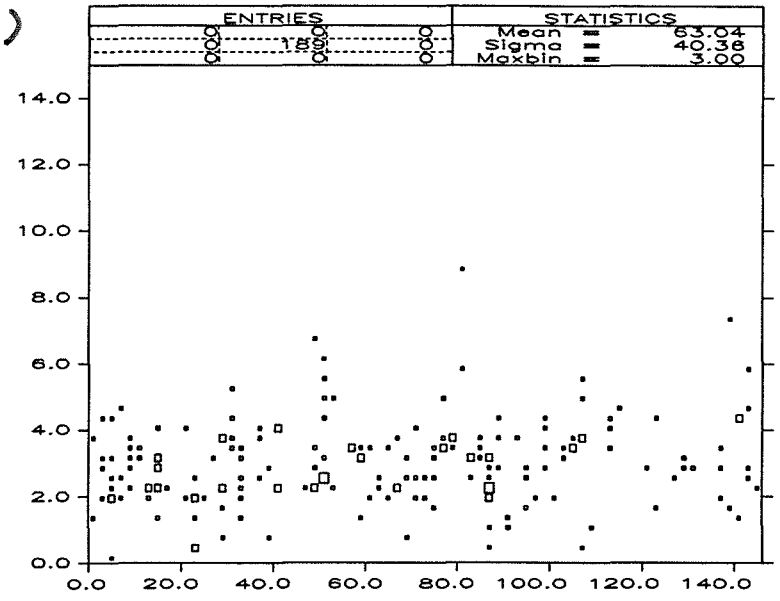

#21020 FHA(Y) VS ETA(X) (W/CUT)

(c)

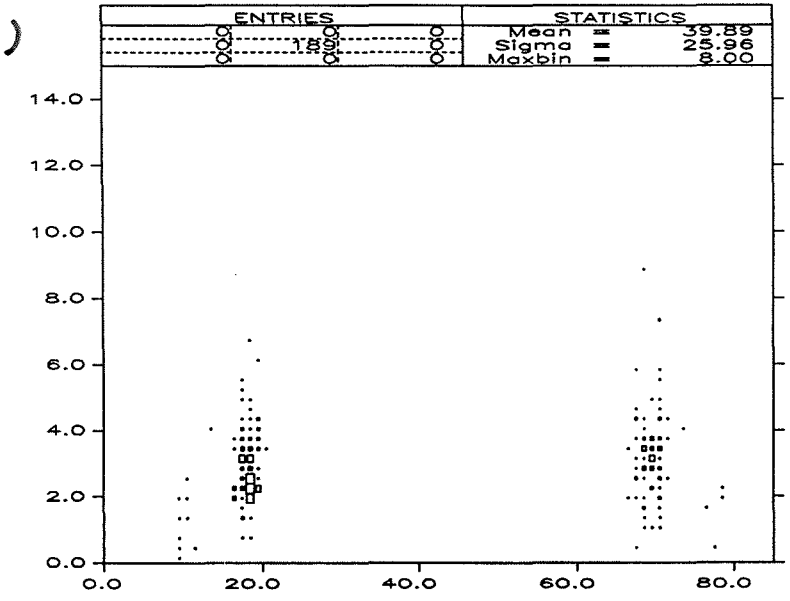

Figures 5(a) – 5(d) 24-MAY-1989 10:42

#21022 MUON PEAK : FHA WEST (W/CUT)

(a)

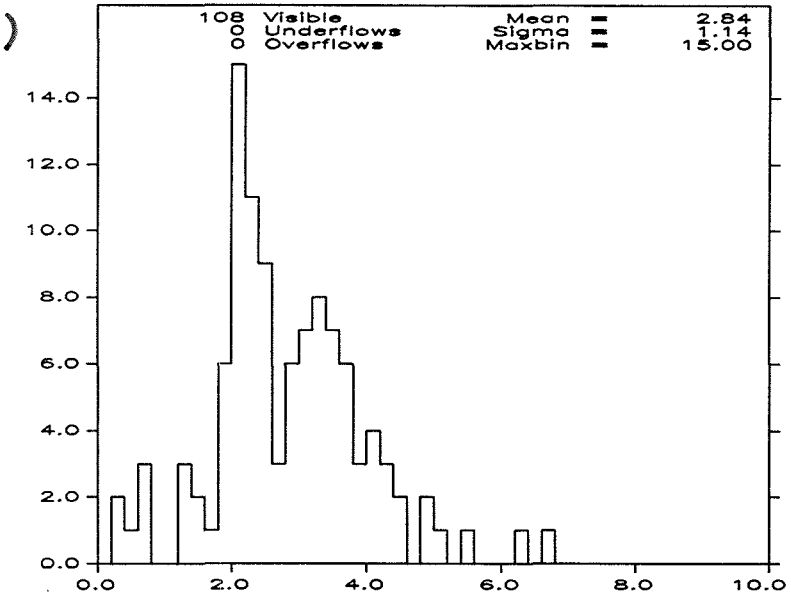

#21023 MUON PEAK : FHA EAST (W/CUT)

(b)

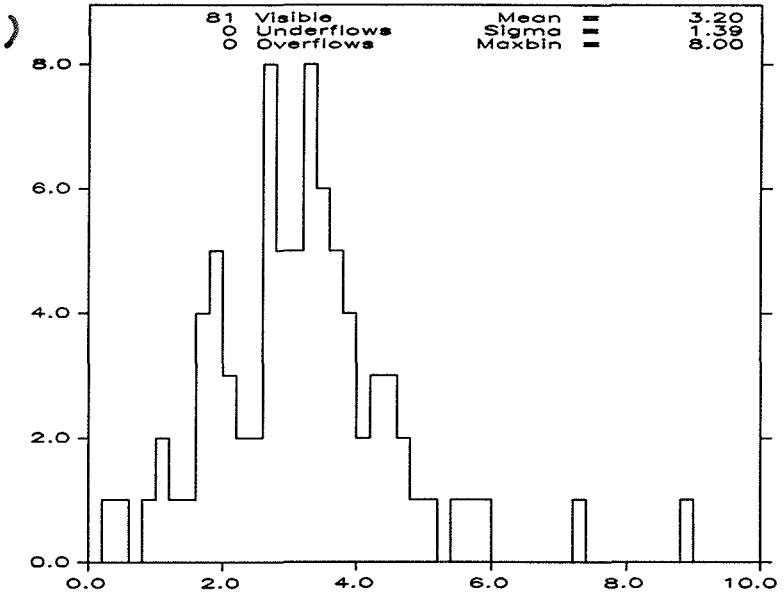

#21039 FHA VS P(MUON) WEST (W/CUT)

(c)

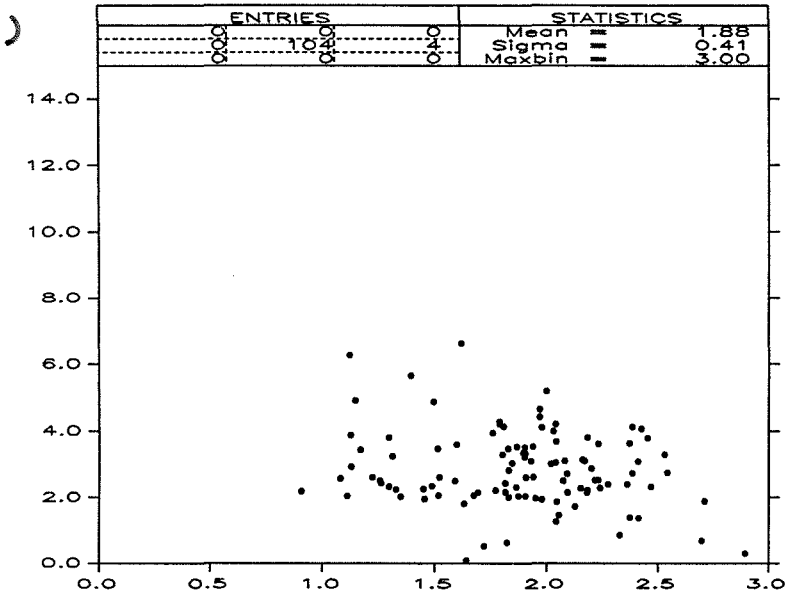

#21040 FHA VS P(MUON) EAST (W/CUT)

(d)

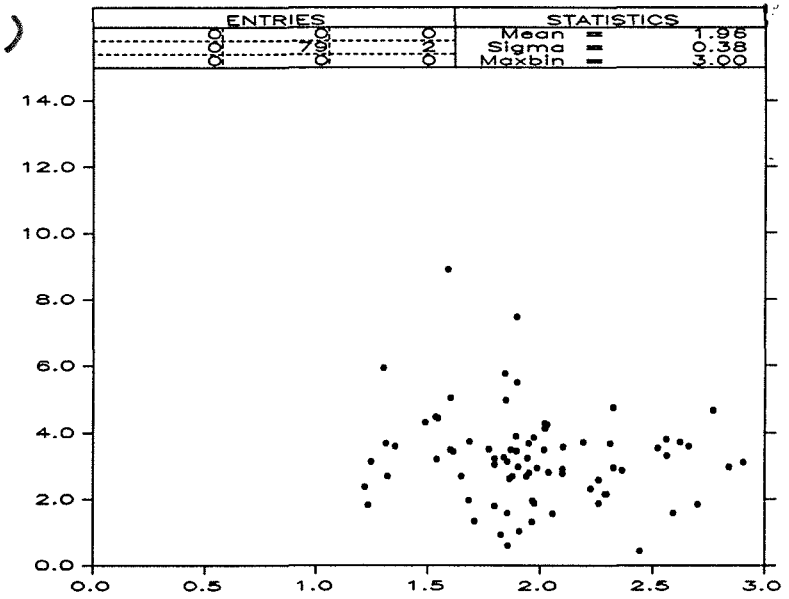

Figures 6(a) – 6(d) 24-MAY-1989 10:44

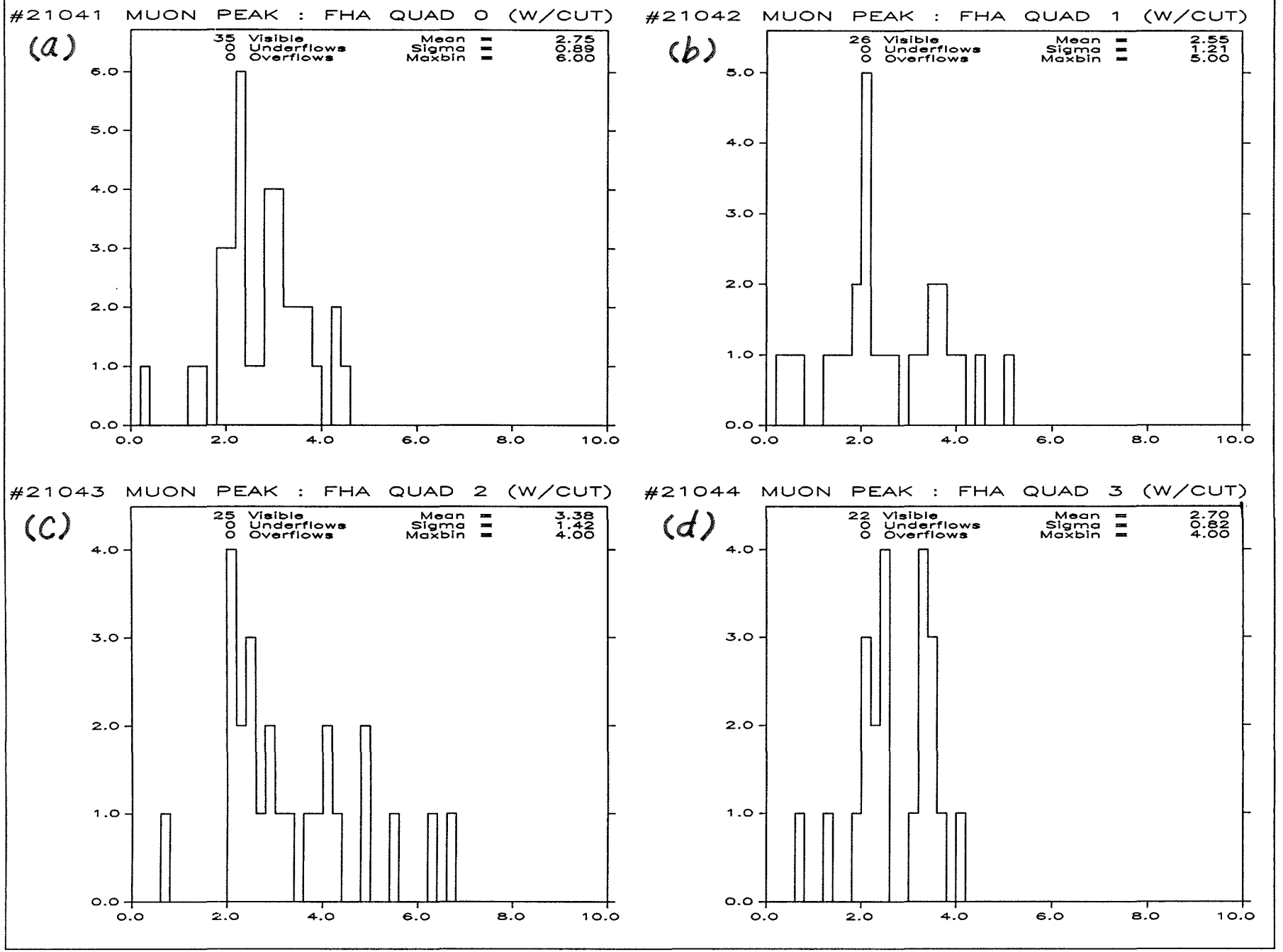

Figures 6(e) – 6(h) 24-MAY-1989 10:46

#21045 MUON PEAK : FHA QUAD 4 (W/CUT)

(e)

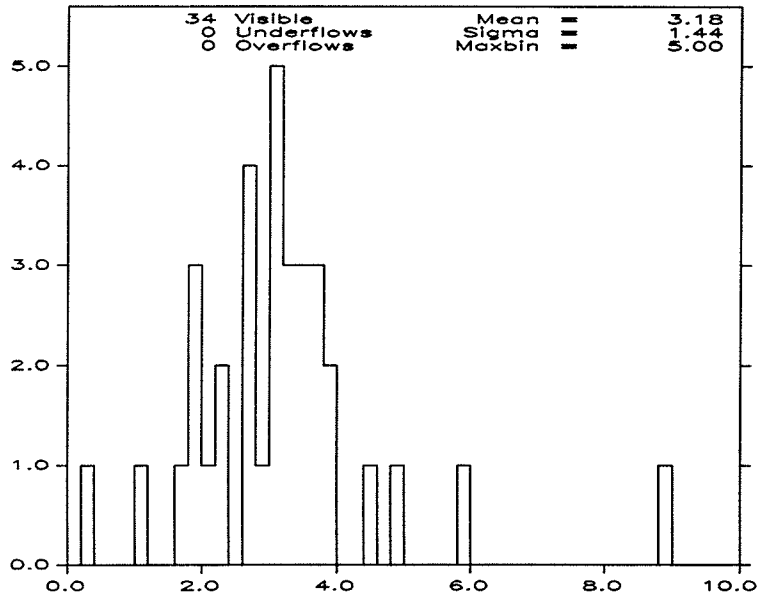

#21046 MUON PEAK : FHA QUAD 5 (W/CUT)

(f)

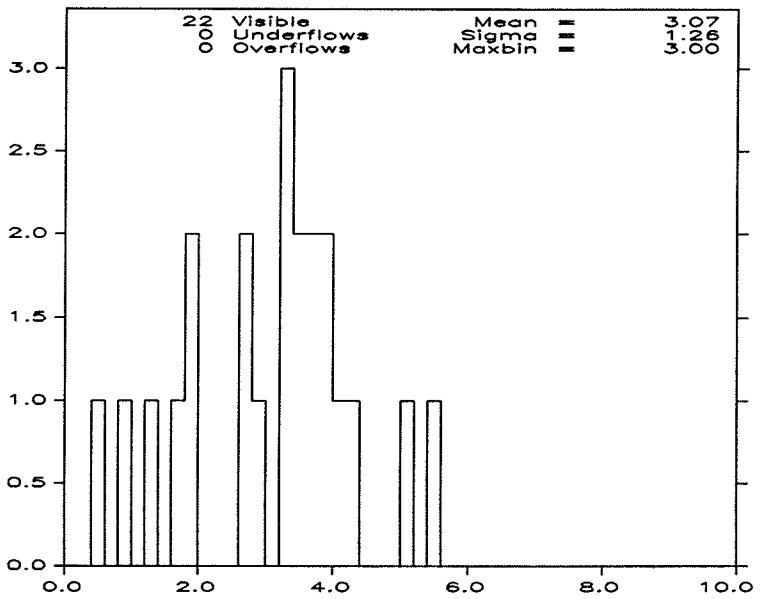

#21047 MUON PEAK : FHA QUAD 6 (W/CUT)

(g)

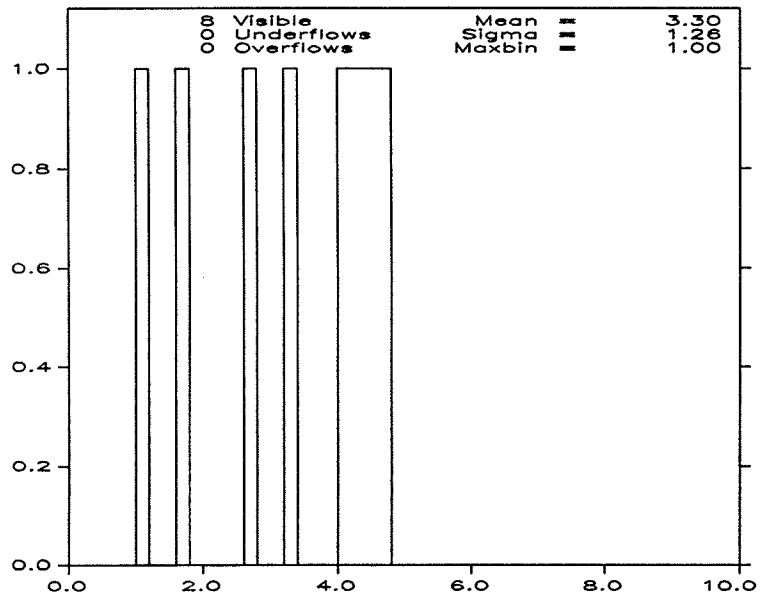

#21048 MUON PEAK : FHA QUAD 7 (W/CUT)

(h)

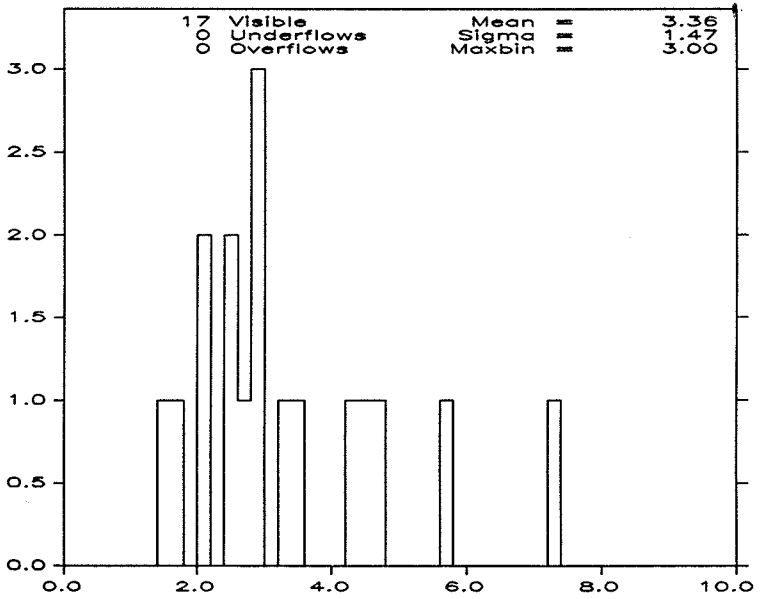

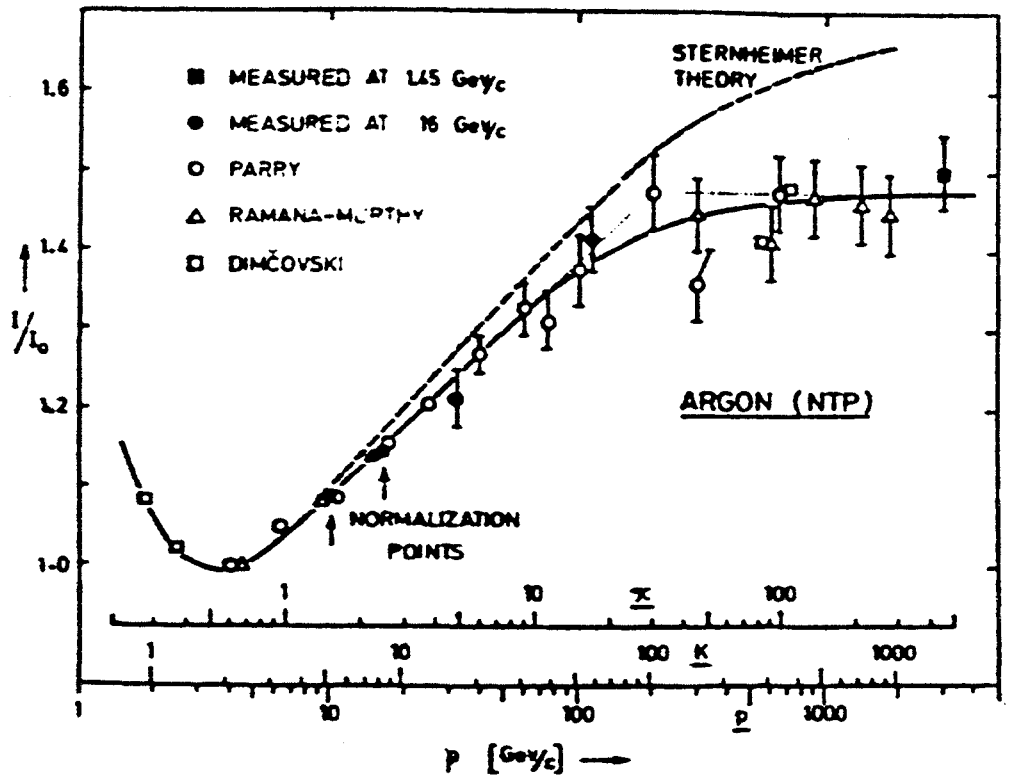

Fig. 7 Relativistic rise of the energy loss in argon, as a function of particle mass and momentum; the vertical scale gives the relative increase above the minimum of ionization[5)]

Figures 8(a) – 8(b) 24-MAY-1989 10:47